Effect of Molecular Weight on the Phase Diagram of Polyethylene under High Pressure

Munehisa YASUNIWA, Kazunao HARAGUCHI,[†] Chitoshi NAKAFUKU,*
and Susumu HIRAKAWA

*Faculty of Science, Fukuoka University,
Jonan-ku, Fukuoka 814-01, Japan*
**Faculty of Education, Kochi University,
Kochi 780, Japan*

ABSTRACT: Differential thermal analysis was performed at pressures from about 400 to 600 MPa to determine the phase diagram of a series of polyethylene from low (2×10^3) to ultra-high molecular weight (2.5×10^6). The different phase diagram was drawn for the high pressure crystallized sample of as-polymerized powder and that of bulk kneaded in the melt at atmospheric pressure. For both samples, the phase transition temperature (T_t) from the extended-chain crystal (orthorhombic) to the high pressure phase (hexagonal) and the melting temperature (T_m) of high pressure phase increase with the molecular weight in the same manner up to the molecular weight about 10^5. Above this molecular weight T_m and T_t of the bulk sample decrease with increasing the molecular weight, while those for the powder sample increase slightly. This decrease of T_m and T_t in the bulk sample is most probably based on entanglements introduced during kneading at atmospheric pressure.
KEY WORDS Polyethylene / High Pressure / DTA / Melting / Crystallization / Molecular Weight / Ultra High Molecular Weight / Phase Diagram / High Pressure Phase /

It is well known that under high pressure above 350 MPa a high pressure phase (hexagonal structure) appears in polyethylene (PE). The high pressure phase was characterized by Takemura *et al.* to be like a liquid crystal using techniques of X-ray diffraction,[1,2] ultrasonic measurement[3] and optical microscopy[4] under high pressure. They have further studied the nature of the phase by Raman spectroscopic measurement and proposed an idea the pressure-induced cross-linking of the PE chain plays a role in the appearance of the phase.[5]

Takamizawa *et al.*[6] have studied the melting and crystallization behavior at 5 kbar by differential thermal analysis (DTA) for the sample of molecular weight (MW) from 6.5×10^3 to 1.3×10^5. According to their results, the high pressure phase begins to appear at the molecular weight above 10^4 and the phase transition temperature (T_t) from so-called "extended-chain crystal" (ECC, orthorhombic structure) to the high pressure phase and the melting temperature (T_m) of the high pressure phase increase with the molecular weight up to 1.3×10^5. Asahi[7] has studied the effect of molecular weight on the phase diagram of low molecular weight polyethylenes (MW: 1000, 2000, 6500, 16000) by X-ray diffraction with a high pressure cell of the diamond-anvil type. Phase diagrams of these samples from 20 to 300°C up to pressures of about 10 kbar has been reported. He has shown that the samples of MW 6500 and 16000 exhibit the high pressure phase, but those of MW 1000 and 2000

---

† Present address: *Y-E DATA Co., Kamifujisawa, Iruma, Saitama 358, Japan.*

don't. Though the phase transition temperatures were almost the same for the samples of MW 6500 and 16000, the melting temperature of the high pressure phase of MW 16000 was higher than that of MW 6500 by 10 or 15°C.

The ultra-high molecular weight PE (UHMW-PE) has been studied by Hoehn *et al.*[8,9] on the crystallization kinetics under high pressure, but the study of the melting process has not been reported. The study of the phase diagram for PE of the whole range of molecular weight is interesting, since the melting behavior under high pressure changes with the molecular weight.[6,7] Several authors[1,4,10-14] have proposed the phase diagrams of PE, however the molecular weight effect on the phase diagram has not been studied. The study of molecular weight effect on the phase diagram proposed by Asahi[7] is in the molecular weight region lower than 16000.

Entanglements should be introduced by kneading in the melt at atmospheric pressure for a high molecular weight polymer. If the pressure-induced cross-linking plays a role on the appearance of the high pressure phase of PE, the entanglements introduced mechanically by kneading at atmospheric pressure may also affect the melting and phase transition behavior of UHMW-PE. Therefore some difference in the melting behavior between the as-polymerized powder sample and the bulk sample kneaded in the melt at atmospheric pressure is expected.

It is the purpose of this paper to describe the phase diagram of PE covering the whole range of molecular weight from 2×10^3 to 2.5×10^6. The effect of sample preparation method at atmospheric pressure on the phase diagram of PE is studied, especially for UHMW-PE.

EXPERIMENTAL

Unfractionated high density polyethylenes were used in this work. Their viscosity-averaged molecular weights are summarized in Table I. Samples 1—5 are commercial poly-

Table I. Molecular weight (viscosity-averaged) of the samples

Sample No.	Molecular weight	Sample No.	Molecular weight
1	2×10^3	6	2.2×10^5
2	4×10^3	7	6.9×10^5
3	1.0×10^4	8	1.6×10^6
4	1.5×10^4	9	2.5×10^6
5	6.7×10^4		

mers supplied by Mitsui Petrochemical Industries Co. The others (samples 6—9) were experimental resins supplied by Showa Denko Co. Molecular weight for samples 6—9 was measured by the supplier from the viscosity of tetralin solution $(0.025 \, \text{g} \, \text{dl}^{-1})$ at 130°C. Samples 1—9 are classified into four groups according to the molecular weight. Samples 1 and 2, samples 3, 4, and 5, samples 6 and 7, and samples 8 and 9 are classified into low, medium, high and ultra-high molecular weight samples (LMW-, MMW-, HMW-, and UHMW-samples), respectively.

Two types of samples, powder and bulk, were used in this experiment. Powder samples were as-polymerized resins. Bulk samples were melt-crystallized (kneaded) ones prepared in the following procedure. In the case of LMW- or MMW-PE a powder sample was kneaded or stirred on a hot plate by a spatula at about 150°C at atmospheric pressure. In the case of HMW- or UHMW-PE a powder sample was melted at about 170°C on the hot plate, and then kneaded by the spatula. As the melt-viscosity was high, a filmy sample could be made by pressing and spreading the melted sample. After folding the filmy sample several times over the sample was kneaded, pressed and spread again. This procedure was performed several times over within about five minutes. Finally the bulk sample was obtained by the rapid cooling of the melted sample to room temperature.

High pressure DTA was carried out by the use of the apparatus described elsewhere.[15] A

rounded heater was set in a high pressure vessel and the sample which was stuck on one of the thermocouple junctions was placed inside of the heater. The heating and cooling rates were precisely controlled by automatic temperature controller. The hydrostatic pressure was measured within ± 1 MPa by a Bourdon gauge (Heise) connected to the high pressure vessel. The powder sample was prepared in the form of a rod (1.2 mm in diameter and 2.5 mm in length) by compressing the original (as-polymerized) sample in the piston-cylinder type cell. The thermocouple for DTA was inserted in the hole which was drilled in the center of the rod. The bulk sample was stucked on the top of the thermocouple in the melt. In order to avoid the effect of pressure transmitting fluid (silicon oil), the samples were coated by epoxy resin.

DTA curves under high pressure were obtained in the following process designated as run 1— run 3 successively. Run 1 is the melting process of the powder or bulk sample prepared at atmospheric pressure (heating rate: 5 K min^{-1}). Run 2 is the crystallization process by slow cooling (cooling rate: 2 K min^{-1}). Run 3 is melting process of the sample crystallized through the process of run 2 (heating rate: 5 K min^{-1}).

In the process of run 1, the sample was heated up to T_h (about 30 K higher temperature than the final peak of DTA melting curve) and held at T_h for two minutes. In the present experiment the final peak of run 1 ends at about 20 K and the crystallization peak of run 2 starts at about 30 K lower temperature than T_h. Consequently the sample was kept in the molten state for about 20 minutes.

RESULTS AND DISCUSSION

The DTA was conducted for all the samples in a series of molecular weights from 2×10^3 to 2.5×10^6 at the pressures of about 400, 500 and 600 MPa.

Figure 1 shows the DTA curves for the bulk
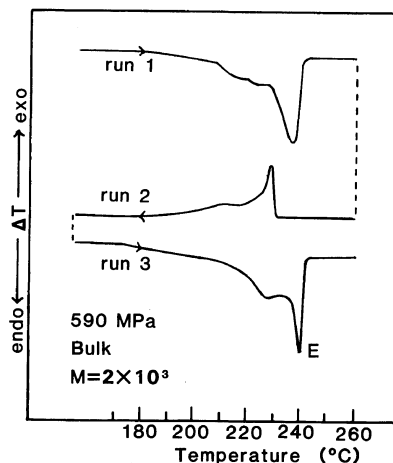

Figure 1. DTA curves of melting and crystallization for the bulk sample of PE of MW 2×10^3 at about 590 MPa. Run 1, melting curve of the sample crystallized from the melt at atmospheric pressure; Run 2, crystallization; Run 3, remelting of the sample crystallized through run 2.

sample with the MW 2×10^3 at 590 MPa. The high pressure crystallized sample shows the similar melting behavior as the sample crystallized from the melt at 1 atm as shown in run 1 and run 3, except for the slight differences of the peak temperatures and the breadth of the peaks of run 1 and run 3. The main endothermic peak of run 3, which is denoted by "E" in the figure, is due to the melting of ECC. The DTA curves for the powder sample of this molecular weight were almost the same as those for the bulk sample. That is, the high pressure crystallized sample, the sample crystallized from the melt at atmospheric pressure and the powder sample show the same melting behavior under high pressure. The origin of the low-temperature shoulder is perhaps due to the melting of the lower molecular weight fraction in the sample.

The DTA curves for the powder and bulk samples were not so different except for the peak height up to MW 2.2×10^5. Above this molecular weight, however, different melting behavior between the powder and bulk samples is observed. Figure 2(a) and (b) show the DTA
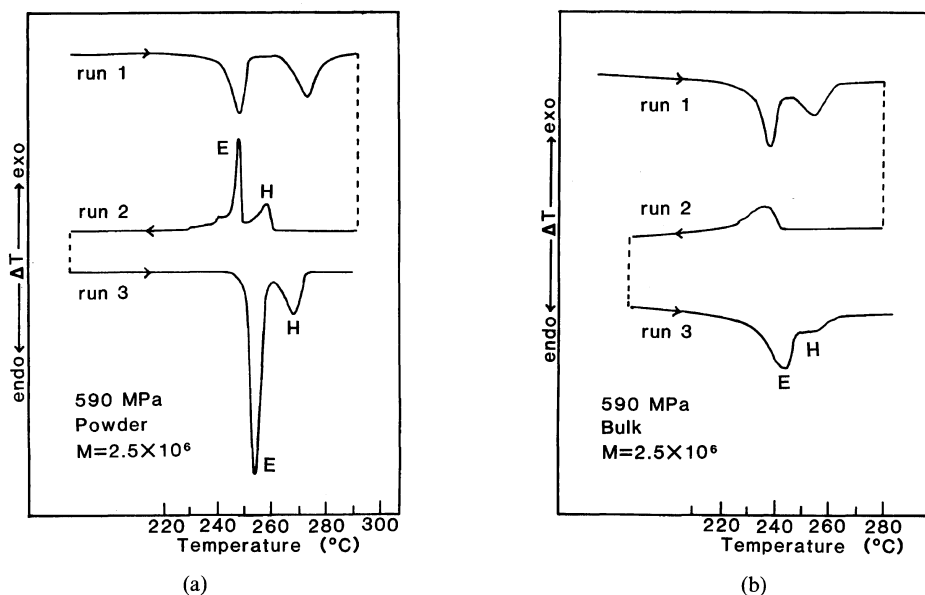
(a)

(b)

Figure 2. DTA curves of melting and crystallization for the powder sample (a) and the bulk sample (b) of PE of MW 2.5×10^6 at about 590 MPa. E, crystallization into ECC in run 2 and melting of ECC in run 3; H, crystallization into the high pressure phase from the melt in run 2 and melting of the high pressure phase in run 3. The processes in each run are the same as in Figure 2.

curves at 590 MPa for the powder and bulk samples with MW 2.5×10^6, respectively. Two sharp and separated peaks appear on the curve for the powder sample, while corresponding two peaks for the bulk sample are broad, especially in run 2. For the bulk sample all the peak temperatures are lower than those for the powder sample, and two peaks in run 2 become single. The low and high temperature peaks in run 3 are assigned to the phase transition from ECC to the high pressure phase and the melting of high pressure phase respectively, as has been reported on the melting of MMW-PE $((4—5) \times 10^4)$.[10,11] The low and high temperature peaks are designated by "E" and "H" respectively. Figure 3 shows the DTA curves of run 3 at 590 MPa for the bulk samples with various molecular weights. A small peak which appears on the high temperature side of the main peak above MW 1.0×10^4 is due to the melting of the high pressure phase. The main peak corresponds to the phase transition from ECC to the high pres-
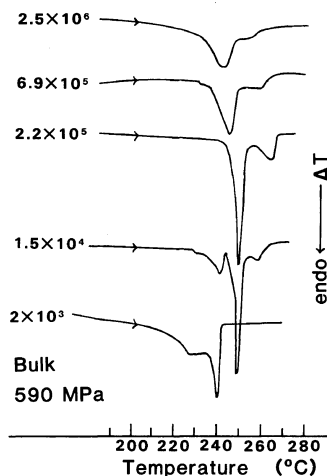

Figure 3. DTA curves of melting at about 590 MPa for the bulk sample with the molecular weight indicated in the figure.

sure phase. Takamizawa *et al.*[6] have also reported the molecular weight dependence of the DTA curves at 5 kbar (490 MPa) for the sample of molecular weight from 6.5×10^3 to

Table II(a). Phase transition temperature (T_t) and melting temperature (T_m)

400 MPa

Molecular weight	Powder sample				Bulk sample			
	T_t		T_m		T_t		T_m	
	P	T	P	T	P	T	P	T
	MPa	°C	MPa	°C	MPa	°C	MPa	°C
2.5×10^6	396	225.5	397	231.5	387	213.0	*	***
1.6×10^6	398	224.8	399	231.0	392	215.0	*	***
6.9×10^5	396	226.5	397	230.0	383	215.0	*	***
2.2×10^5	395	225.3	*	***	393	223.5	*	***
6.7×10^4	403	225.3	*	***	400	223.8	*	***
1.5×10^4	405	223.3	*	***	399	220.5	*	***
1.0×10^4	402	219.5	*	***	397	216.3	*	***
4×10^3	399	216.3	*	***	375	207.0	*	***
2×10^3	403	213.0	*	***	402	211.3	*	***

500 MPa

Molecular weight	Powder sample				Bulk sample			
	T_t		T_m		T_t		T_m	
	P	T	P	T	P	T	P	T
	MPa	°C	MPa	°C	MPa	°C	MPa	°C
2.5×10^6	496	238.3	498	248.8	502	231.5	501	239.0
1.6×10^6	491	239.5	493	249.8	490	229.0	492	238.0
6.9×10^5	485	238.5	487	248.3	496	231.5	498	242.5
2.2×10^5	512	240.8	514	251.0	500	238.5	502	248.0
6.7×10^4	495	240.3	496	246.5	498	238.8	500	248.8
1.5×10^4	499	237.5	*	***	502	237.5	*	***
1.0×10^4	464	225.8	*	***	496	236.3	*	***
4×10^3	506	233.8	*	***	496	232.0	*	***
2×10^3	496	228.0	*	***	493	221.5	*	***

1.3×10^5. The result obtained by them is in accordance with the present one substantially, though the dependence in the UHMW region have not been studied. The peak temperatures of the DTA curves in Figure 3 increase with increasing the molecular weight up to MW 2.2×10^5. Above this molecular weight, however the peak temperatures of the DTA curves decrease with increasing the molecular weight, and the peaks become broad. On the other hand, for the powder sample almost the same DTA curves as that of MW 2.2×10^5 was obtained even above this molecular weight. This result indicates that in UHMW region the melting behavior for the bulk sample is different from that of the powder sample.

As pressure in the pressure vessel changed slightly with temperature by thermal expansion of pressure transmitting fluid, the pressure where the DTA peak was observed was mea-

Table II(a). continued

600 MPa

Molecular weight	Powder sample				Bulk sample			
	T_t		T_m		T_t		T_m	
	P	T	P	T	P	T	P	T
	MPa	°C	MPa	°C	MPa	°C	MPa	°C
2.5×10^6	596	254.0	600	269.0	588	244.0	588	255.0
1.6×10^6	591	253.5	596	269.5	587	243.0	588	256.0
6.9×10^5	604	254.0	606	269.3	588	246.0	591	260.0
2.2×10^5	592	253.0	596	268.5	592	250.0	596	265.0
6.7×10^4	599	255.8	603	267.8	599	251.8	603	267.0
1.5×10^4	591	251.0	593	259.3	588	249.0	590	259.0
1.0×10^4	598	249.0	602	257.0	593	249.8	596	257.0
4×10^3	592	249.5	*	***	586	246.0	597	253.5
2×10^3	596	241.5	*	***	586	240.0	*	***

Table II(b). Phase transition temperature (T_t') and crystallization temperature (T_c)

400 MPa

Molecular weight	Powder sample				Bulk sample			
	T_t'		T_c		T_t'		T_c	
	P	T	P	T	P	T	P	T
	MPa	°C	MPa	°C	MPa	°C	MPa	°C
2.5×10^6	386	219.3	387	222.8	387	205.5	*	***
1.6×10^6	387	217.5	388	220.8	388	208.3	*	***
6.9×10^5	392	220.8	*	***	380	208.5	*	***
2.2×10^5	388	219.8	*	***	389	217.5	*	***
6.7×10^4	387	217.3	*	***	397	217.0	*	***
1.5×10^4	402	216.0	*	***	392	213.3	*	***
1.0×10^4	397	210.5	*	***	379	205.0	*	***
4×10^3	395	206.5	*	***	371	195.8	*	***
2×10^3	393	199.8	*	***	403	200.3	*	***

sured for each peak. Table II lists the peak temperatures, T_m, T_t, T_c (crystallization temperature from the melt to the high pressure phase), and T_t' (phase transition temperature from high pressure phase to ECC), and pressures where corresponding peaks appear. When the peak of melting or crystallization of the high pressure phase was unable to separate from main peak in the DTA curves, the column of the list is filled by the mark of *.

The phase diagram of PE between about 400 and 600 MPa was determined by the plot of the peak temperatures of T_m, T_t, T_c, and T_t'. Figure 4(a) and (b) show the melting phase diagram under high pressure for the powder and bulk samples of MW 2.2×10^5 and

Table II(b). continued

500 MPa

Molecular weight	Powder sample				Bulk sample			
	T'_t		T_c		T'_t		T_c	
	P	T	P	T	P	T	P	T
	MPa	°C	MPa	°C	MPa	°C	MPa	°C
2.5×10^6	496	234.0	497	238.8	499	226.5	*	***
1.6×10^6	489	234.0	491	239.5	490	224.5	*	***
6.9×10^5	484	234.8	485	240.3	496	226.5	*	***
2.2×10^5	505	236.3	506	239.5	496	233.0	498	236.3
6.7×10^4	480	232.3	481	236.3	505	235.3	506	239.3
1.5×10^4	490	231.8	*	***	499	232.8	*	***
1.0×10^4	463	218.0	*	***	505	231.5	*	***
4×10^3	502	224.5	*	***	491	222.8	*	***
2×10^3	498	216.5	*	***	488	210.8	*	***

600 MPa

Molecular weight	Powder sample				Bulk sample			
	T'_t		T_c		T'_t		T_c	
	P	T	P	T	P	T	P	T
	MPa	°C	MPa	°C	MPa	°C	MPa	°C
2.5×10^6	592	248.3	595	258.5	585	236.3	*	***
1.6×10^6	591	247.5	594	259.5	584	236.0	*	***
6.9×10^5	605	250.7	607	258.5	585	239.0	*	***
2.2×10^5	593	249.5	595	258.5	588	246.0	592	252.0
6.7×10^4	596	249.0	597	254.5	601	247.8	603	259.5
1.5×10^4	600	246.5	601	250.0	588	244.0	588	247.8
1.0×10^4	599	244.0	*	***	588	245.0	588	246.3
4×10^3	584	241.3	*	***	584	239.5	*	***
2×10^3	596	230.5	*	***	583	228.8	*	***

2.5×10^6, respectively. In the HMW-PE, the phase transition line (T_t line) and the melting line (T_m line) are not so different between the powder and bulk samples. For UHMW-PE, however, both T_m and T_t lines for the bulk sample shift to the lower temperature than those for the powder sample. That is, the high pressure phase region for the bulk sample which is shown by the dotted area in the phase diagram shifts to the lower temperature than that of the powder sample. The peak temperatures of T_c and T'_t also shift to the low temperature side for the bulk sample, as shown in Figure 5(a) and (b). As shown in run 2 of Figure 2(b), the exothermic peak is very broad. The exothermic peak of the crystallization from the melt to the high pressure phase does not appear separately, therefore T_c line of the UHMW-PE bulk sample can not be drawn in Figure 5(b).
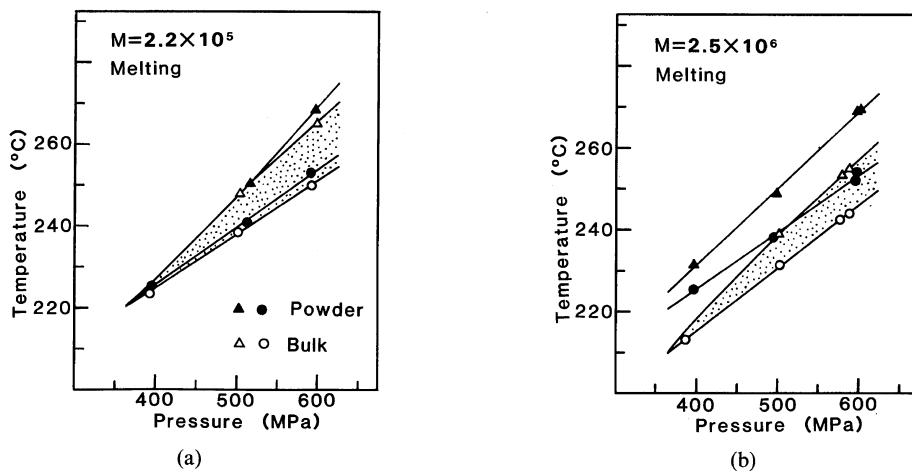
Figure 4. Phase diagrams of melting of PE of MW 2.2×10^5 (a) and 2.5×10^6 (b). $\bigcirc$, $\bullet$, phase transition from ECC to high pressure phase, $\triangle$, $\blacktriangle$, melting of the high pressure phase.
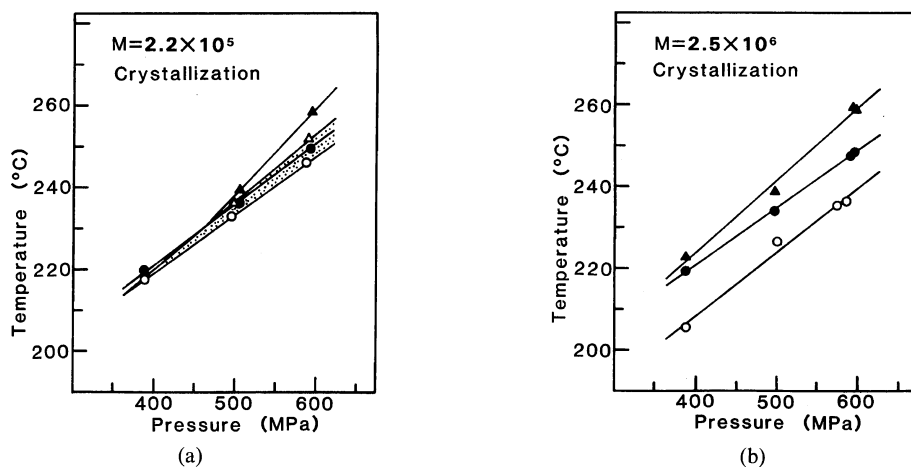

Figure 5. Phase diagrams of crystallization of PE of MW 2.2×10^5 (a) and 2.5×10^6 (b). The symbols are the same as in Figure 4.

As shown in Figures 4 and 5, T_m, T_t, T_c, and T_t' lines are approximately straight lines. Accordingly, the pressure dependences of T_m, T_t, T_c, and T_t' were approximated by a linear equation which was obtained by the method of least squares. By the use of the linear equation, the calibrated values T_m, T_t, T_c, and T_t' at a given pressure between 350—650 MPa can be obtained. Table III lists the calibrated T_m, T_t, T_c, and T_t' at the pressure of 500 MPa and pressure dependences $\mathrm{d}T_m/\mathrm{d}p$, $\mathrm{d}T_t/\mathrm{d}p$, $\mathrm{d}T_c/\mathrm{d}p$,

and $\mathrm{d}T_t'/\mathrm{d}p$ in the region of 400—600 MPa for all the molecular weight samples.

The molecular weight dependences of T_m and T_t at 600 MPa for the powder and bulk samples are shown in Figure 6. The T_m increases monotonically with the molecular weight in the low to medium molecular weight region. The T_m and T_t increase with the molecular weight up to about 10^5 for both samples, and in the case of the powder sample the gradual increase of T_m and

Table III(a). Calibrated melting (T_m) and transition (T_t) temperatures at 500 MPa

Molecular weight	$T_m/°C$		$T_t/°C$	
	Powder	Bulk	Powder	Bulk
2.5×10^6	250.2	238.8	239.5	230.6
1.6×10^6	250.3	239.4	239.7	230.4
6.9×10^5	249.9	242.8	240.7	232.4
2.2×10^5	248.0	247.6	239.7	238.0
6.7×10^4	247.3	248.8	240.6	238.3
1.5×10^4	***	***	237.3	235.8
1.0×10^4	***	***	233.3	234.9
4×10^3	***	***	233.3	231.0
2×10^3	***	***	227.7	225.2

Table III(b). Calibrated crystallization (T_c) and transition (T_t') temperatures at 500 MPa

Molecular weight	$T_c/°C$		$T_t'/°C$	
	Powder	Bulk	Powder	Bulk
2.5×10^6	241.5	***	235.0	224.2
1.6×10^6	241.6	***	234.4	224.7
6.9×10^5	243.9	***	236.6	226.6
2.2×10^5	238.2	236.6	235.9	233.4
6.7×10^4	239.3	238.0	234.7	233.2
1.5×10^4	***	***	231.7	230.5
1.0×10^4	***	***	226.5	229.0
4×10^3	***	***	225.2	223.0
2×10^3	***	***	216.2	214.7

Pressure dependences of melting (dT_m/dp) and transition (dT_t/dp) temperatures in the region of 400—600 MPa

Molecular weight	dT_m/dp (K/100 MPa)		dT_t/dp (K/100 MPa)	
	Powder	Bulk	Powder	Bulk
2.5×10^6	18.7	18.3	13.9	15.5
1.6×10^6	19.0	18.7	14.4	14.3
6.9×10^5	18.4	18.8	13.4	15.1
2.2×10^5	21.2	18.1	14.0	13.3
6.7×10^4	19.9	17.7	15.5	14.1
1.5×10^4	**	**	14.5	14.5
1.0×10^4	**	**	15.4	17.1
4×10^3	**	**	17.2	18.5
2×10^3	**	**	14.7	15.5

Pressure dependences of crystallization (dT_c/dp) and transition (dT_t'/dp) temperatures in the region of 400—600 MPa

Molecular weight	dT_c/dp (K/100 MPa)		dT_t'/dp (K/100 MPa)	
	Powder	Bulk	Powder	Bulk
2.5×10^6	17.6	**	14.0	15.7
1.6×10^6	18.8	**	14.5	14.1
6.9×10^5	13.2	**	13.9	14.8
2.2×10^5	21.3	16.7	14.5	14.3
6.7×10^4	15.6	20.8	15.1	15.1
1.5×10^4	**	**	15.1	14.8
1.0×10^4	**	**	17.0	19.2
4×10^3	**	**	18.3	20.5
2×10^3	**	**	15.1	15.9

T_t is observed up to MW 2.5×10^6. For the bulk sample, however, both T_m and T_t decrease with increasing the molecular weight above 2.2×10^5.

At atmospheric pressure, the melting temperature also increases with increasing the molecular weight. The dependence of the melting temperature on the reciprocal molecular weight has been expressed by a linear equation.[16] The dependences of T_m and T_t for the powder sample on the reciprocal molecular weight at 600 MPa also resulted in the expression of a linear equation. Takamizawa et al.[6] have reported that T_m and T_t in the heating process at 490 MPa increase with increasing

the molecular weight up to MW 1.3×10^5. Then they have calculated molecular weight dependence of melting temperature and estimated equilibrium melting temperature. The melting temperature for the powder sample of MW 2.5×10^6 at 498 MPa become 250°C which is still 3°C lower than the estimated equilibrium melting temperature at this pressure.

For the UHMW bulk sample, the DTA peaks of the melting and transition are small and broad, and the peak temperatures are lower than those of the powder sample, as is seen in the comparison of the DTA curves of
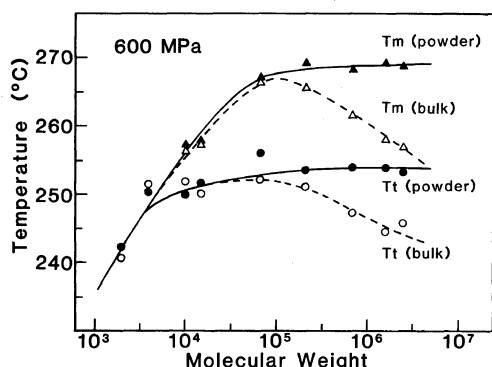
Figure 6. Molecular weight dependences of the phase transition temperature (T_t) from ECC to high pressure phase and the melting temperature (T_m) of the high pressure phase of PE. ○, ●, phase transition from ECC to high pressure phase, △, ▲, melting of the high pressure phase.

Figure 2(a) and (b). The origin of the difference of the melting behavior between the powder and bulk samples may be interpreted as follows. In the bulk sample, chain entanglements may be introduced mechanically during kneading of a sample in the melt at atmospheric pressure. Smith et al.[17,18] have suggested that for the quenched UHMW-PE all entanglements existing in the melt were trapped during solidification process. Accordingly it is considered that mechanically introduced entanglements should be trapped in the bulk sample. Since the molecular chain of UHMW-PE is longer than the lamellar thickness of ECC, chain disentangling during crystallization under high pressure may not occur easily on the time scale of the present DTA experiment. That is, the quantity of the trapped entanglements may not decrease drastically in the crystallization process under high pressure. The entanglements may hinder the crystal growth and bring defects in the crystal, therefore the quantity of the small and disordered crystals should increase by the kneading in the UHMW bulk sample. As a matter of course, the small and disordered crystals give the decrease in the melting temperature and the broad and small melting peak. On the other hand, the as-polymerized powder sample may scarcely include such entanglements. That is, it is supposed that the difference of the melting behavior between the powder and bulk samples is due to the entanglements of long chain molecule. The analysis of small angle X-ray scattering and the morphorogical investigation by scanning electron microscopy suggest that the small and disordered crystals are formed by high pressure crystallization in the UHMW bulk sample.[19]

REFERENCES

1. M. Yasuniwa, R. Enoshita, and T. Takemura, *Jpn. J. Appl. Phys.*, **15**, 1421 (1976).
2. K. Matsushige and T. Takemura, *J. Cryst. Growth*, **48**, 343 (1980).
3. K. Nagata, K. Tagashira, S. Taki, and T. Takemura, *Jpn. J. Appl. Phys.*, **19**, 985 (1980).
4. M. Yasuniwa and T. Takemura, *Polymer*, **15**, 661 (1974).
5. H. Tanaka and T. Takemura, *Polym. J.*, **12**, 355 (1980).
6. K. Takamizawa, Y. Urabe, A. Oono, and T. Takemura, Abstracts of Papers, SPSJ 22nd Symposium, Tokyo, November 8, 1973, p 1—447.
7. T. Asahi, *J. Polym. Sci., Polym. Phys. Ed.*, **22**, 175 (1984).
8. H. H. Hoehn, R. C. Ferguson, and R. R. Hebert, *Polym. Eng. Sci.*, **18**, 457 (1978).
9. R. C. Ferguson and H. H. Hoehn, *Polym. Eng. Sci.*, **18**, 466 (1978).
10. D. C. Bassett and B. Turner, *Nature (Phys. Sci.).*, **240**, 146 (1972).
11. M. Yasuniwa, C. Nakafuku, and T. Takemura, *Polym. J.*, **4**, 526 (1973).
12. T. Yamamoto, H. Miyaji, and K. Asai, *Jpn. J. Appl. Phys.*, **16**, 1891 (1977).
13. M. Hikosaka, S. Minomura, and T. Seto, *Jpn. J. Appl. Phys.*, **19**, 1763 (1980).
14. Y. Maeda, H. Kanetsuna, K. Nagata, K. Matsushige, and T. Takemura, *J. Polym. Sci., Polym. Phys. Ed.*, **19**, 1313 (1981).

15. N. Hiramatsu and S. Hirakawa, *Polym. J.*, **12**, 105 (1980).
16. B. Wunderlich, "Macromolecular Physics," Vol. 3, Academic Press, New York, N. Y., 1980, Section 8.5.1.
17. P. Smith, P. J. Lemstra, and H. C. Booij, *J. Polym. Sci., Polym. Phys. Ed.*, **19**, 877 (1981).
18. P. Smith, *Macromolecules*, **16**, 1802 (1983).
19. M. Yasuniwa, C. Nakafuku, and S. Hirakawa, in preparation.